



Open Research Online

The Open University's repository of research publications
and other research outputs

Forecasting multivariate road traffic flows using Bayesian dynamic graphical models, splines and other traffic variables

Journal Item

How to cite:

Anacleto Junior, Osvaldo; Queen, Catriona and Albers, Casper (2013). Forecasting multivariate road traffic flows using Bayesian dynamic graphical models, splines and other traffic variables. Australian & New Zealand Journal of Statistics, 55(2) pp. 69–86.

For guidance on citations see [FAQs](#).

© 2013 Australian Statistical Publishing Association Inc.

Version: Accepted Manuscript

Link(s) to article on publisher's website:
<http://dx.doi.org/doi:10.1111/anzs.12026>

Copyright and Moral Rights for the articles on this site are retained by the individual authors and/or other copyright owners. For more information on Open Research Online's data [policy](#) on reuse of materials please consult the policies page.

oro.open.ac.uk

Forecasting multivariate road traffic flows using Bayesian dynamic graphical models, splines and other traffic variables

Oswaldo Anacleto*

Department of Mathematics and Statistics, The Open University

Catriona Queen

Department of Mathematics and Statistics, The Open University

Casper Albers

Department of Psychometrics and Statistics, University of Groningen

Abstract

Traffic flow data are routinely collected for many networks worldwide. These invariably large data sets can be used as part of a traffic management system, for which good traffic flow forecasting models are crucial. The linear multiregression dynamic model (LMDM) has been shown to be promising for forecasting flows, accommodating multivariate flow time series, while being a computationally simple model to use. While statistical flow forecasting models usually base their forecasts on flow data alone, data for other traffic variables are also routinely collected. This paper shows how cubic splines can be used to incorporate extra variables into the LMDM in order to enhance flow forecasts. Cubic splines are also introduced into the LMDM to parsimoniously accommodate the daily cycle exhibited by traffic flows.

The proposed methodology allows the LMDM to provide more accurate forecasts when forecasting flows in a real high-dimensional traffic data set. The resulting extended LMDM can deal with some important traffic modelling issues not usually considered in flow forecasting models. Additionally the model can be implemented in a real-time environment, a crucial requirement for traffic management systems designed to support decisions and actions to alleviate congestion and keep traffic flowing.

Keywords: linear multiregression dynamic model, dynamic linear model, state space models, cubic splines, occupancy, headway, speed.

*Corresponding author (o.anacleto-junior@open.ac.uk). The authors thank the Highways Agency for providing the data used in this paper and also Les Lyman from Mott MacDonald for valuable discussions on preliminary data analyses. The authors also would like to thank two Referees for their constructive and helpful comments on an earlier version of the paper.

1 Introduction

Traffic flow data are routinely collected across many traffic networks worldwide. These data sets are invariably very large with variables measured at a number of data collection sites $S(1), \dots, S(n)$, very often collected minute-by-minute over long periods of time. These time series data can be used as part of a traffic management system to assess highway facilities and performance over time or to monitor and control traffic flows in real-time. They can also be used as part of a traveller's information system. The success of such systems relies on good short-term forecasting models of flows and it is the development of such models which is considered in this paper.

Despite the fact that traffic flow data are invariably multivariate — often of high dimension — many authors model the flow at each site in isolation. However, the flows at upstream and downstream sites are very informative about the flows at $S(i)$ and there are substantial gains to be made by using this information when forecasting flows. Some authors (Tebaldi *et al.*, 2002; Kamarianakis and Prastacos, 2005; Stathopoulos and Karlaftis, 2003) do use other flows to help forecast flows at each $S(i)$, while others (Whittaker *et al.*, 1997; Sun *et al.*, 2006) additionally use conditional independence so that only the flows at sites adjacent to $S(i)$ are required to help forecast flows at $S(i)$. However, these authors use lagged flows, whereas, as shown in Anacleto *et al.* (2013), when the distances between sites are such that vehicles are counted at several different sites within the same time period — as they are in the network considered in this paper — then using information regarding *contemporaneous* flows can greatly improve forecast performance.

Following the traffic flow modelling ideas of Queen *et al.* (2007), Queen and Albers (2009) and Anacleto *et al.* (2013), this paper uses a multivariate Bayesian dynamic graphical model called the linear multiregression dynamic model (LMDM) (Queen and Smith, 1993) to forecast flows. Instead of using lagged flow information, the LMDM uses contemporaneous upstream flow information at time t to forecast flows at site $S(i)$ *at the same time t* (by marginalising the forecast distribution for $S(i)$ at time t - see Section 3 for details). The LMDM can accommodate the high-dimensional, often complex, multivariate relationships which can exist between flow series across networks, and yet, because it uses a graph to decompose the problem into smaller, simpler sub problems, it is a computationally simple

model to use, making it an ideal candidate for on-line traffic forecasting.

Statistical flow forecasting models usually base their forecasts on flow data alone. However, data for other traffic variables — namely, occupancy, headway and speed — are also routinely collected for many roads. Each of these variables has a non-linear relationship with flow. This paper investigates how cubic splines can be used to incorporate these extra traffic variables into the LMDM. The paper also introduces the use of cubic splines within the LMDM to accommodate seasonal patterns, and in particular, to accommodate the daily cycle exhibited by traffic flows. The proposed models are used in the paper to forecast traffic flows at a busy motorway intersection near Manchester, UK.

Although the paper focuses on the problem of forecasting traffic flows, the proposed model has much wider applicability to any application involving multivariate time series which exhibits a causal structure and, as such, the methodology presented in the paper is of interest in its own right.

The paper is structured as follows. Section 2 describes the data used throughout the paper. Section 3 gives a brief review of the LMDM and describes how cubic splines can be used within the LMDM in order to accommodate the daily cycle exhibited by traffic flows. In Section 4, cubic splines are also used to model the non-linear relationships which exist between the extra traffic variables and flows. These cubic splines are then incorporated into the LMDM so that information regarding the extra traffic variables can be used when forecasting flows. Section 5 goes on to assess the forecast performance of these models, while Section 6 offers some concluding remarks.

2 The data

This paper focuses on forecasting traffic flows at the intersection of three motorways — the M60, M62 and M602 — west of Manchester, UK. Figure 1(a) shows a schematic diagram of the network with arrows showing the direction of travel and circles indicating the data collection sites. The data used in the paper were collected in 2010 by the Highways Agency in England (<http://www.highways.gov.uk/>).

FIGURE 1 ABOUT HERE

The flow data for this network are minute counts of vehicles passing over inductive loops

in the surface of the road at each site (for a brief description of the data collection process by inductive loops, see Li, 2009). Even though minute counts are available, because of the high variability of these, researchers usually aggregate the data (Vlahogianni *et al.*, 2004 and Chandra and Al-Deek, 2009). Anacleto *et al.* (2013), who developed models for forecasting flows in this same Manchester network using the same data as here, aggregated the flows into 15-minute intervals, making the data and their models particularly useful for assessing highway facilities and for providing traveller information. In this paper, the focus is on real-time traffic control for which 5-minute intervals are suitable, and so the data will be aggregated into 5 minute intervals here.

Figure 1(b) shows 5-minute flow time series plots for sites 9206B and 1437A for a typical week. Notice the morning and afternoon peaks at both sites, which are also evident at all other sites in the network. As was shown in Anacleto *et al.* (2013), flows in this network vary in level and variability for different weekdays. These differences can be incorporated into the model, but for clarity, in this paper only data for Wednesdays are considered. Further, the very low overnight flows (which are of little interest for real-time traffic control) are ignored and only data between 06:00-20:59 are used.

As mentioned in the introduction, the distances between sites in this network are such that vehicles are usually counted at several data sites in the same 5-minute interval. As a result, the flows at sites upstream to site $S(i)$ at time t are helpful in forecasting the flows at $S(i)$ at the same time t . It would, of course, be easier to use lagged upstream flows (which are known at time t) for forecasting at time t rather than contemporaneous upstream flows (which are not known at time t). However, Anacleto *et al.* (2013) found that for both 15-minute and 5-minute data in this network, a model which used contemporaneous upstream flows within an LMDM performed better than a model using lagged flows.

In addition to the flow data, there are data for three other variables collected at each site:

- Occupancy: the percentage of time that vehicles are ‘occupying’ the inductive loop;
- Headway: the average time between vehicles passing over the inductive loop (in sec);
- (Time mean) speed: the average ratio of the distance between two (consecutive) inductive loops in a road segment and the time taken by each vehicle to pass over these

FIGURE 2 ABOUT HERE

loops (in kph).

These data are available minute-by-minute and averaged into 5-minute values for considering with 5-minute flow data.

3 The model

This section describes the LMDM used for 5-minute flow data in the Manchester network. For a detailed description of the LMDM, see Queen and Smith (1993).

Denote the flow at $S(i)$ during time period t by $Y_t(i)$. Suppose that there are conditional independence relationships related to causality across $Y_t(1), \dots, Y_t(n)$ so that for each $Y_t(i)$, $i = 2, \dots, n$, there is a set of variables, $pa(Y_t(i)) \subseteq \{Y_t(1), \dots, Y_t(i-1)\}$, for which, conditional on the set of variables $pa(Y_t(i))$, $Y_t(i)$ is independent of $\{Y_t(1), \dots, Y_t(i-1)\} \setminus pa(Y_t(i))$ (where “ \setminus ” reads “excluding”). These relationships can be represented by a directed acyclic graph (DAG) in which there are directed arcs to $Y_t(i)$ from each variable in $pa(Y_t(i))$. Each variable in $pa(Y_t(i))$ is known as a *parent* of $Y_t(i)$ while $Y_t(i)$ in turn is a *child* of each variable in $pa(Y_t(i))$. If $pa(Y_t(i)) = \emptyset$, then $Y_t(i)$ is known as a *root node*.

In Anacleto *et al.* (2013), a DAG was elicited for the Manchester network using the directions of traffic flows and possible routes through the network: the final DAG used in that paper, which will also be used in this paper, is shown in Figure 2.

The LMDM uses the DAG to model the n -dimensional multivariate time series by n separate (conditional) univariate Bayesian regression dynamic linear models (DLMs) (West and Harrison, 1997). Let D_{t-1} denote the information available at time $t-1$. Then the LMDM is defined as follows for all times $t = 1, 2, \dots$:

$$Y_t(i) = \mathbf{F}_t(i)^\top \boldsymbol{\theta}_t(i) + v_t(i), \quad v_t(i) \sim N(0, V_t(i)), \quad i = 1, \dots, n, \quad (1)$$

$$\boldsymbol{\theta}_t = \mathbf{G}_t \boldsymbol{\theta}_{t-1} + \mathbf{w}_t, \quad \mathbf{w}_t \sim N(\mathbf{0}, \mathbf{W}_t), \quad (2)$$

$$\boldsymbol{\theta}_{t-1} | D_{t-1} \sim N(\mathbf{m}_{t-1}, \mathbf{C}_{t-1}). \quad (3)$$

where the vector $\mathbf{F}_t(i)$ contains an arbitrary, but known, function of the parents $pa(Y_t(i))$ and possibly other known variables; $\boldsymbol{\theta}_t(i)$ is the state vector associated with $Y_t(i)$ and $\boldsymbol{\theta}_t^\top =$

$(\boldsymbol{\theta}_t(1)^\top \cdots \boldsymbol{\theta}_t(n)^\top)$; $v_t(1), \dots, v_t(n)$ are the observation errors, $V_t(1), \dots, V_t(n)$ are the scalar observation variances; the square matrices $\mathbf{G}_t = \text{blockdiag}(\mathbf{G}_t(1) \cdots \mathbf{G}_t(n))$ and $\mathbf{W}_t = \text{blockdiag}(\mathbf{W}_t(1) \cdots \mathbf{W}_t(n))$ are such that $G_t(i)$ and $W_t(i)$ are, respectively, the state evolution matrix and evolution covariance matrix for $\boldsymbol{\theta}_t(i)$; $\mathbf{w}_t^\top = (\mathbf{w}_t(1)^\top \cdots \mathbf{w}_t(n)^\top)$ where $\mathbf{w}_t(i)$ is the system error vector for $Y_t(i)$; $\mathbf{0}$ is a vector of zeros; and vector \mathbf{m}_{t-1} and square matrix $\mathbf{C}_{t-1} = \text{blockdiag}(\mathbf{C}_{t-1}(1) \cdots \mathbf{C}_{t-1}(n))$ are the posterior moments for $\boldsymbol{\theta}_{t-1}$. The errors $v_t(1), \dots, v_t(n)$ and $\mathbf{w}_t(1), \dots, \mathbf{w}_t(n)$ are mutually independent of each other and through time.

At each time t , given the posterior distribution for $\boldsymbol{\theta}_{t-1}|D_{t-1}$ in (3), the prior for $\boldsymbol{\theta}_t|D_{t-1}$ is obtained via the system equation (2) and, in turn, the forecast distribution for each $Y_t(i)|pa(Y_t(i)), D_{t-1}$ is obtained from the observation equations (1). The block diagonal forms of \mathbf{W}_t and \mathbf{G}_t ensure that if the state vectors are initially mutually independent, then they remain so for all time t . Basically, the LMDM specifies n separate (conditional) univariate models — one each for $Y_t(1)$ and $Y_t(i)|pa(Y_t(i)), i = 2, \dots, n$ — where each $Y_t(i)$ has a function of its parents as linear regressors and its associated state vector, $\boldsymbol{\theta}_t(i)$, is updated separately in closed form in $Y_t(i)$'s (conditional) univariate model. Root nodes without parents are modelled by any suitable univariate DLM.

From (1), the forecast distribution for each $Y_t(i)|pa(Y_t(i))$ is normal and can be obtained separately within the LMDM. However, as $Y_t(i)$ and $pa(Y_t(i))$ both represent flows at the same time t , the *marginal* forecasts for each $Y_t(i)$ are required. Although the marginal forecast distributions cannot generally be calculated analytically, the marginal forecast moments are readily available using $E[Y_t(i)] = E\{E[Y_t(i)|pa(Y_t(i))]\}$ and $V[Y_t(i)] = E\{V[Y_t(i)|pa(Y_t(i))]\} + V\{E[Y_t(i)|pa(Y_t(i))]\}$. Essentially, in the LMDM, the marginal forecast moments of flows at upstream sites are used to obtain the marginal forecast moments for $Y_t(i)$, which in turn are used to find the marginal forecast moments of sites further downstream, and so on (see Queen and Smith, 1993 and Queen *et al.*, 2008).

The observation variances $V_t(1), \dots, V_t(n)$ in (1) are estimated on-line as data are observed using a method proposed by Anacleto *et al.* (2013) to accommodate the heteroscedasticity exhibited by time series of traffic flows. Briefly, each $V_t(i)$ is replaced by

$$V_t(i) = \exp\{\alpha \log[E(Y_t(i)|D_{t-1})]\}\phi_t(i)^{-1} \quad (4)$$

where α is such that

$$\log(\text{variance of flow}) = \alpha \log(\text{mean flow})$$

and can be estimated using historical data (this relationship is different for the two periods 7.00pm–6.59am and 7.00am–6.59pm and so α takes one value for t between 7.00pm and 6.59am each day, and a different value between 7.00am and 6.59pm); $E(Y_t(i)|D_{t-1})$ is the one-step ahead forecast mean for $Y_t(i)$; and $\phi_t(i)$ is the underlying observation precision which is estimated on-line using the discounting variance learning techniques described in West and Harrison (1997), page 359.

The matrices $\mathbf{W}_t(1), \dots, \mathbf{W}_t(n)$ are also estimated on-line using standard DLM discounting techniques (see West and Harrison, 1997, page 193).

Because of the heteroscedasticity of traffic flow time series, when evaluating model forecast performance it is important to consider the performance of the precision of forecasts as well as point forecasts. Thus, a measure which assesses the accuracy of the multivariate forecast distribution as a whole, rather than just the point forecasts, is preferred. Such a measure is the joint log-predictive likelihood (LPL). After observing the time series up to time T , the LPL evaluates the log of the density of the joint one-step ahead forecast distribution at time t at the observed value $\mathbf{y}_t^\top = (y_t(1), \dots, y_t(n))$, and aggregates these over all values $t = 1, \dots, T$. In the LMDM, because of the conditional independence structure across $Y_t(1), \dots, Y_t(n)$, the density of the joint one-step ahead forecast distribution at time t evaluated at the observed value \mathbf{y}_t is given by

$$f(\mathbf{y}_t|D_{t-1}) = \prod_{i=1}^n f(y_t(i)|pa(y_t(i)), D_{t-1})$$

where $f(y_t(i)|pa(y_t(i)), D_{t-1})$ is the one-step forecast density for $Y_t(i)$ conditional on its parents, evaluated at $y_t(i)$. Thus, the LPL for the LMDM is calculated as

$$\text{LPL} = \sum_{t=1}^T \left[\sum_{i=1}^n \log\{f(y_t(i)|pa(y_t(i)), D_{t-1})\} \right]. \quad (5)$$

The larger the value of the LPL, the more support there is for the corresponding model. The forecast densities in (5) are calculated at time $t - 1$ *before* $y_t(i)$ is observed. Therefore, the LPL is not subject to overfitting problems which may affect model comparison.

3.1 Modelling the daily cycle

In the LMDM of Anacleto *et al.* (2013), the daily cycle observed in flows at root nodes was modelled using a seasonal factor representation so that $\boldsymbol{\theta}_t(i)$ in (1) is a 96-dimensional vector of flow level parameters (one mean flow level parameter for each 15-minute period in the day) with corresponding 96-dimensional vector $\mathbf{F}_t(i)^\top = (1 \ 0 \ \dots \ 0)$. (The matrix \mathbf{G}_t in (2) then ‘cycles’ through the mean level parameters to ensure that the correct 15-minute mean flow level parameter is used at time t .) Child series have their parents as linear regressors, where the regression coefficients represent the proportions of vehicles flowing from parent to child. These proportions also exhibit a daily pattern, also modelled by a seasonal factor representation in Anacleto *et al.* (2013) so that, for a series with a single parent (for simplicity), once again $\boldsymbol{\theta}_t(i)$ in (1) is a 96-dimensional vector of proportion parameters with corresponding 96-dimensional vector $\mathbf{F}_t(i)^\top = (pa(y_t(i)) \ 0 \ \dots \ 0)$.

Unfortunately, when the dimension of the state vector gets large, numerical problems can arise when updating the variances associated with a DLM (Prado and West, 2010). This can be tackled by using alternative equations in the Kalman filter algorithm, as implemented in the *R DLM* package (Petrís *et al.*, 2009), but when dealing with 5-minute data, the dimension of the state vector is so large (12×24) that it becomes important to consider alternatives to the seasonal factor representation to keep model parsimony. Following Tebaldi *et al.* (2002), to address this problem splines can be used to represent daily cycles in each univariate DLM within the LMDM.

Cubic splines are widely used in regression models in order to relax the linearity assumption for continuous regressors (see Harrell, 2001, and Hastie *et al.*, 2001). A cubic spline has the basic form:

$$f(x) = \sum_{m=1}^M \beta_m h_m(x), \quad (6)$$

where $h_m(x) = x^m$ for $m = 1, 2, 3$ and $h_m(x) = (x - k_{m-3})^3$ for $m = 4, \dots, M$ for values k_1, \dots, k_{M-3} with $a < k_1 < k_2 < \dots < k_{M-3} < b$, where $[a, b] \in \mathbb{R}$ is the domain of x . When $x - k_{m-3}$ is negative, then $h_m(x) = 0$. The functions $h_1(x), \dots, h_M(x)$ are called spline basis functions, k_1, \dots, k_{M-3} are the spline knots and β_1, \dots, β_M are parameters. In the context of regression, the idea is to consider the spline basis functions as regressor variables and then estimate the parameters β_1, \dots, β_M .

In a dynamic LMDM context, a similar approach can be used. Consider a root node. The daily cycle can be modelled in a time series using a spline to fit one full cycle. In this case, x would be time t and k_1, \dots, k_{M-3} would represent times over the cycle. For example, for 5-minute data with a daily cycle over 24 hours, k_1 could be 13, for example, representing the time period 01:00–01:04 and t would be the current time (which at 02:00–02:04, say, would be $t = 25$). Prior data can be used to calculate the spline basis functions $h_1(x), \dots, h_M(x)$ which can then be evaluated at each 5-minute time period $x = t$. The regression vector $\mathbf{F}_t(i)$ for root node $Y_t(i)$ in (1) then has the form:

$$\mathbf{F}_t(i)^\top = (h_1(t) \ \cdots \ h_M(t)). \quad (7)$$

(This form of $\mathbf{F}_t(i)$ only models the daily cycle of flows: it is possible that $\mathbf{F}_t(i)$ could have additional elements, for example there may be other exogenous regressors for $Y_t(i)$'s DLM.) For $\mathbf{F}_t(i)$ in (7), the associated state vector in (1) is:

$$\boldsymbol{\theta}_t(i)^\top = (\beta_{t1} \ \cdots \ \beta_{tM}) \quad (8)$$

where $\beta_{t1}, \dots, \beta_{tM}$ are dynamic versions of the associated parameters in (6), which evolve through the system equation (2) with state evolution matrix $\mathbf{G}_t(i)$ being the M -dimensional identity matrix.

Although Harrell (2001) suggests that the positions of k_1, \dots, k_{M-3} are not important when fitting splines for static regression purposes, it was found that LMDMs for traffic flows give better results when concentrating the positions of k_1, \dots, k_{M-3} during morning and afternoon peak periods. Harrell (2001) also recommends using only 3 to 5 knots for static regression. However, when using splines to represent daily cycles of flows, 15 to 20 knots were typically found to perform much better. This is a small number when compared to the 288 parameters required to use a seasonal factor representation to model 5-min flow data. Moreover, overfitting is controlled because fitted splines were found to not vary very much over time and the parameters $\beta_{t1}, \dots, \beta_{tM}$ evolve dynamically to capture any drift in time.

Example 1

Suppose that the daily cycle of root node $Y_t(1)$ is to be represented by a spline with (for simplicity) just two knots, k_1 and k_2 , and that an exogenous regressor, X_t , is also to be

included in $Y_t(1)$'s DLM. Then the observation equation for $Y_t(1)$ has the form

$$Y_t(1) = \sum_{m=1}^5 \beta_{tm} h_m(t) + \alpha_t x_t + v_t(1), \quad v_t(1) \sim N(0, V_t(1)),$$

so that in (1),

$$\begin{aligned} \mathbf{F}_t(1)^\top &= (h_1(t) \cdots h_5(t) \ x_t) \\ \boldsymbol{\theta}_t(1)^\top &= (\beta_{t1} \cdots \beta_{t5} \ \alpha_t). \end{aligned}$$

In this case the evolution matrix $\mathbf{G}_t(1) = \text{blockdiag}(\mathbf{I}_5, g)$ where \mathbf{I}_5 is the 5-dimensional identity matrix and g is some scalar in \mathbb{R} for parameter α_t 's evolution. \square

A child in the LMDM is modelled as having its parents as linear regressors. For example, if $Y_t(3)$ has parents $Y_t(1)$ and $Y_t(2)$, then the simplest observation equation for $Y_t(3)$ would be

$$Y_t(3) = \alpha_t(1)y_t(1) + \alpha_t(2)y_t(2) + v_t(3), \quad v_t(3) \sim N(0, V_t(3))$$

so that $\mathbf{F}_t(3)^\top = (y_t(1) \ y_t(2))$ and $\boldsymbol{\theta}_t(3)^\top = (\alpha_t(1) \ \alpha_t(2))$. For traffic flow data, the regression parameters ($\alpha_t(1)$ and $\alpha_t(2)$ in the example above) exhibit a daily pattern (see, for example, Anacleto *et al.*, 2013). A spline can be used to model the daily cycle by setting each regression parameter to the form $\sum_{m=1}^M \beta_{tm} h_m(t)$. Thus, in general the regression and state vectors $\mathbf{F}_t(i)$ and $\boldsymbol{\theta}_t(i)$ for child variable $Y_t(i)$ with (for simplicity) single parent $pa(Y_t(i))$ have the forms:

$$\mathbf{F}_t(i)^\top = (pa(y_t(i))h_1(t) \cdots pa(y_t(i))h_M(t)), \quad (9)$$

$$\boldsymbol{\theta}_t(i)^\top = (\beta_{t1} \cdots \beta_{tM}). \quad (10)$$

Again, $\boldsymbol{\theta}_t(i)$ evolves through the system equation (2) with state evolution matrix $\mathbf{G}_t(i)$ being the M -dimensional identity matrix. As with the splines for root nodes, it was found that splines with 15 to 20 knots performed best and, again, overfitting is not a issue since the parameters in (10) are estimated as flows are observed and the proportion splines do not vary much over time.

Example 2

Suppose that $Y_t(3)$ has parents $Y_t(1)$ and $Y_t(2)$ and the daily cycles exhibited by $Y_t(1)$ and $Y_t(2)$'s regression parameters are to be represented by splines with three and two knots,

respectively. Suppose further that an exogenous regressor, Z_t , is also to be included in $Y_t(3)$'s model. Then the observation equation for $Y_t(3)$ has the form

$$Y_t(3) = y_t(1) \sum_{m=1}^6 \beta_{tm}^{(1)} h_m(t)^{(1)} + y_t(2) \sum_{m=1}^5 \beta_{tm}^{(2)} h_m(t)^{(2)} + \gamma_t z_t + v_t(3), \quad v_t(3) \sim N(0, V_t(3)),$$

so that in (1),

$$\begin{aligned} \mathbf{F}_t(3)^\top &= (h_1(t)^{(1)} \ \dots \ h_6(t)^{(1)} \ h_1(t)^{(2)} \ \dots \ h_5(t)^{(2)} \ z_t) \\ \boldsymbol{\theta}_t(3)^\top &= (\beta_{t1}^{(1)} \ \dots \ \beta_{t6}^{(1)} \ \beta_{t1}^{(2)} \ \dots \ \beta_{t5}^{(2)} \ \gamma_t). \end{aligned}$$

In this case the evolution matrix $\mathbf{G}_t(3) = \text{blockdiag}(\mathbf{I}_6, \mathbf{I}_5, g)$ where \mathbf{I}_k is the k -dimensional identity matrix and g is some scalar in \mathbb{R} for parameter γ_t 's evolution. \square

To take advantage of the computational simplicity of a fully conjugate LMDM, normal priors need to be specified for the state vectors. When using the seasonal factor model for modelling the daily cycle exhibited by regression parameters in the child model (as in Anacleto *et al.*, 2013), the regression parameters are proportions and so normal priors are not ideal. However, when using splines to model the regression parameters' daily cycles (as in this paper), using normal priors is not a problem as the spline regression parameters do not have any restrictions on their values.

In order to compare the performance of using cubic splines and seasonal factors for modelling daily cycles in the LMDM, both models were used to forecast four separate bivariate series formed by considering the four root nodes (in Figure 2) together with one of their children each: specifically, the four bivariate series considered were $(Y_t(9206B), Y_t(9200B))$, $(Y_t(6013B), Y_t(6007L))$, $(Y_t(9188A), Y_t(9193J))$ and $(Y_t(1431A), Y_t(1437A))$. To also assess whether dynamic estimation of the spline parameters $\beta_{t1}, \dots, \beta_{tM}$ (as in (8) and (10)) improves forecast performance, forecasts for these four bivariate series were also obtained using a static version of the cubic spline LMDM, by using a system equation (2) with no error term \mathbf{w}_t .

Observed flows from July to August 2010 were used to estimate the spline basis functions, form priors for all state vectors and to estimate parameter α for each $V_t(i)$ in equation (4) for these three models (so that each model had the same equivalent priors). One-step ahead forecasts for flows were then obtained for September 2010.

TABLE 1 ABOUT HERE

Each model and each series requires two separate discount factors to be specified: one for estimating $\phi_t(i)$ in (4) and one for estimating \mathbf{W}_t . Usually these discount factors are chosen by comparing the forecast accuracy of different models varying discount factor values (as suggested by West and Harrison, 1997). However, the high number of models and the level of complexity makes this optimization a demanding task. For example, the optimization of the combination of both discount factors for \mathbf{W}_t and $\phi_t(i)$ for a child time series would depend on the optimization of the discount factors for \mathbf{W}_t and $\phi_t(i)$ in its parent. Due to this, based on preliminary tests, the chosen value for the discount factors for both \mathbf{W}_t and $\phi_t(i)$ in all models in this paper was 0.99.

Table 1 shows the LPLs for the three models for each bivariate series. The number of spline basis functions for static and dynamic spline LMDMs varied between 15 and 20 among the considered time series, and the LPL values shown in Table 1 are for the number of basis functions which performed best for each model and each series. In Table 1, the dynamic spline versions of the LMDMs produce the largest LPL values for all bivariate series, indicating that the dynamic spline LMDMs provide the most accurate forecasts.

An alternative parsimonious approach to using cubic splines for modelling the daily cycle would be to use a Fourier representation, as in West and Harrison (1997), Section 8.6. The standard Fourier representation can be used directly for modelling the daily cycle exhibited by the parents, but the model would need to be adapted somewhat for modelling the daily cycle in the proportion regression parameters in the models for child variables. When modelling the four root nodes, however, the Fourier representation was found to perform worse than both the seasonal factor model and the splines, and so Fourier models were not pursued further.

4 Traffic variables as predictor variables in the LMDM

As mentioned in Section 2, the data collection process used by the Highways Agency in England includes real-time measurement of flow, together with occupancy, speed and headway. Although there is great interest and an extensive literature concerning traffic flow modelling, few models deal with the analysis of flow in conjunction with the other variables. Based on a

FIGURE 3 ABOUT HERE

survey carried out by Vlahogianni *et al.* (2004), of forty traffic models where flow was considered, just seven used other extra variables, while none considered all three. From a statistical perspective, Ahmed and Cook (1979) and Levin and Tsao (1980) fitted independent ARIMA models for flow and occupancy forecasting, while Whittaker *et al.* (1997) tackled a similar problem using state space models. Neural networks have also been used for modelling flow in conjunction with other variables, for example in Innamaa (2000), Abdulhai *et al.* (1999) and Gilmore and Abe (1995). Multivariate forecasting of flow, speed and occupancy using k -nearest neighbour classifiers has also been considered by Clark (2003). More recently, Chandra and Al-Deek (2009) considered vector autoregressive models to forecast flows using speed as a predictor variable.

In this section, occupancy, speed and headway data will be incorporated into the LMDM to enhance flow forecasts.

4.1 Relationships between flows and other traffic variables

The first row of Figure 3 shows scatterplots of flow at time t versus occupancy at previous time $t - 1$ at site 9188A for three separate months. The plots indicate an increasing relationship between flow and occupancy until the latter reaches some value around 20, which is usually defined by traffic managers as the road capacity and varies from site to site. For occupancy values higher than this road capacity, the relationship then turns to be decreasing, which can lead to congestion. This relationship, first observed by Greenshields (1935), is well known in the traffic literature and is usually called the fundamental diagram of traffic (for details, see Ashton, 1966).

Scatterplots of flow at time t versus headway at previous time $t - 1$ at the same site for the same three months are shown in the second row of Figure 3. These plots confirm an intuitive relationship in the sense that the flow decreases as the average time between cars increases.

The last row of Figure 3 shows scatterplots of flow at time t versus speed at previous time $t - 1$, again at site 9188A for the same three months. Most flow values are concentrated at speed values between 80 kph and 100 kph, with an apparently decreasing relationship in

this region. There also seems to be an increasing relationship between flow at t and speed at $t - 1$ for low speed values, although with a slightly higher level of variability: it is likely that many of these points are from situations where congestion occurred.

In the LMDM, exogenous variables can be easily introduced into the model as regressors (as X_t and Z_t were in the earlier examples). Figure 3 suggests non-linear relationships between flow and all the possible predictor variables of interest. Plots of flow at t versus the other traffic variables at $t - 1$ look broadly comparable at the other sites. Adopting a similar approach used when modelling the daily flow cycle described in Section 3, splines can be used to model the non-linear relationships between flow at time t and the exogenous variables at time $t - 1$. These splines can then be incorporated into the LMDM as regressors.

For traffic control, it is preferable to include all three of the splines (for occupancy, speed and headway) as regressors for forecasting flows. This is because one predictor variable may be better for predicting possible changes in flow behaviour (such as congestion) than other predictors at one time, and a different variable may be better for predicting possible changes in flow at another time. Thus, although the model with all three predictors may not necessarily be the most parsimonious, it will be more responsive to traffic conditions and so, from a practical point of view, will be the most useful model for traffic control. Additionally, the fact that certain regressors give the best forecast performance on the data considered in this paper is not a guarantee that the same regressors will give the best performance for *future* data. Therefore, the focus of this paper is to present a model which uses all three predictors rather than searching for a subset of predictors which performs best for this particular dataset.

This paper only considers using the values of the traffic variables at time $t - 1$ for forecasting flows at time t . Different lags could be used, so that values of the traffic variables at time $t - k$, for $k > 1$, could be used instead of, or in addition to, $t - 1$. Whichever lags are used, splines can still be used to model the relationships between the traffic variables at $t - k$ and flow at t , and the same methods proposed in this paper can then be used to incorporate these splines into the LMDM as regressors.

4.2 Incorporating the predictor variables in the LMDM

Consider a bivariate time series $(Y_t(1), Y_t(2))$, representing the flows at sites $S(1)$ and $S(2)$, where $Y_t(1)$ is a root node and $pa(Y_t(2)) = Y_t(1)$. Since $Y_t(1)$ is a root node, the regression and state vectors for $Y_t(1)$ when using cubic splines to model the daily cycle in the LMDM are given by (7) and (8), respectively. Suppose that occupancy at time $t - 1$ at site $S(1)$ is to be used for forecasting $Y_t(1)$ and that a cubic spline (6) represents the relationship between occupancy at $S(1)$ at time $t - 1$ and $Y_t(1)$ with basis functions $h_1^{O_1}(t - 1), \dots, h_{M_1}^{O_1}(t - 1)$ and associated parameters $\beta_{t1}^{O_1}, \dots, \beta_{tM_1}^{O_1}$. Then, an LMDM can be defined so that the regression vector (7) is augmented to

$$\mathbf{F}_t(1)^\top = (h_1(t) \cdots h_M(t) \ h_1^{O_1}(t - 1) \cdots h_{M_1}^{O_1}(t - 1)) \quad (11)$$

and the associated state vector (8) is augmented to

$$\boldsymbol{\theta}_t(1)^\top = (\beta_{t1} \cdots \beta_{tM} \ \beta_{t1}^{O_1} \cdots \beta_{tM_1}^{O_1}). \quad (12)$$

As usual, $\boldsymbol{\theta}_t(1)$ evolves through the system equation (2) with state evolution matrix $\mathbf{G}_t(1)$ being the $(M + M_1)$ -dimensional identity matrix. Similarly, the basis functions and parameters for cubic splines representing the relationships between $Y_t(1)$ and headway and speed at $S(1)$ at $t - 1$ can also be included in (11) and (12), respectively.

To use occupancy at site $S(2)$ at $t - 1$ for forecasting child $Y_t(2)$, suppose that $h_1^{O_2}(t - 1), \dots, h_{M_2}^{O_2}(t - 1)$ and $\beta_{t1}^{O_2}, \dots, \beta_{tM_2}^{O_2}$ are the basis functions and associated parameters of the cubic spline representing the relationship between occupancy at time $t - 1$ and flow at time t at site $S(2)$. Based on the regression and state vectors for a child in the LMDM given in (9) and (10),

$$\begin{aligned} \mathbf{F}_t(2)^\top &= (y_t(1)h_1(t) \cdots y_t(1)h_M(t) \ h_1^{O_2}(t - 1) \cdots h_{M_2}^{O_2}(t - 1)), \\ \boldsymbol{\theta}_t(2)^\top &= (\beta_{t1} \cdots \beta_{tM} \ \beta_{t1}^{O_2} \cdots \beta_{tM_2}^{O_2}). \end{aligned}$$

State vector $\boldsymbol{\theta}_t(2)$ evolves through the system equation (2) with state evolution matrix $\mathbf{G}_t(2)$ being the $(M + M_2)$ -dimensional identity matrix. The basis functions and parameters for cubic splines representing the relationships between $Y_t(2)$ and headway and speed at $S(2)$ at $t - 1$ can similarly be included in $\mathbf{F}_t(2)$ and $\boldsymbol{\theta}_t(2)$.

The extension to the case where a child has more than one parent is straightforward. For example, consider the scenario of Example 2 in which $Y_t(3)$ has parents $Y_t(1)$ and $Y_t(2)$, where the daily cycle for the regression parameters is represented by splines with three knots for $Y_t(1)$ and two knots for $Y_t(2)$, and exogenous variable Z_t needs to be included in $Y_t(3)$'s model. Then a spline representing the relationship between occupancy at time $t - 1$ and flow at time t at site $S(3)$ can be additionally incorporated into the model by setting

$$\begin{aligned}\mathbf{F}_t(3)^\top &= (h_1(t)^{(1)} \dots h_6(t)^{(1)} \ h_1(t)^{(2)} \dots h_5(t)^{(2)} \ z_t \ h_1^{O_3}(t-1) \dots h_{M_3}^{O_3}(t-1)) \\ \boldsymbol{\theta}_t(3)^\top &= (\beta_{t1}^{(1)} \dots \beta_{t6}^{(1)} \ \beta_{t1}^{(2)} \dots \beta_{t5}^{(2)} \ \gamma_t \ \beta_{t1}^{O_3} \dots \beta_{tM_3}^{O_3}).\end{aligned}$$

In this case the evolution matrix $\mathbf{G}_t(3) = \text{blockdiag}(\mathbf{I}_6, \mathbf{I}_5, g, \mathbf{I}_{M_3})$ where \mathbf{I}_k is the k -dimensional identity matrix and g is some scalar in \mathbb{R} for parameter γ_t 's evolution.

The black lines in Figure 3 are the fitted cubic splines for each of the presented scatterplots. Unlike the splines fitted for the daily flow cycle in Section 3, in this case the position of the spline knots did not have a considerable effect on the final curve. Also, as suggested by Harrell (2001), four knots were used as a default for fitting all the splines representing extra traffic variables used in the LMDM.

A comparison of the scatterplots between the columns of Figure 3 suggests that the relationships between flow at time t and the predictor variables at time $t - 1$ do not vary very much over time. As a consequence, spline fitting would not have to be updated on a frequent basis. However, even if frequent spline fitting were required, fitting is computationally very quick, so it could be used in real-time. Similar conclusions are valid when looking at the same scatterplots for traffic data collected at other months during 2010 and also for different data collection sites. This is also very useful because it means that huge amounts of data are not required before the models can be used.

In this paper, as mentioned in Section 2, only forecasts for Wednesdays are considered. In a model for all weekdays, it would be parsimonious to have a single spline for all days of the week. In fact, preliminary data analysis indicates that splines fitted using data from Wednesdays and splines fitted using all weekdays give similar results. What's more, the forecast performance of the two models using these two sets of splines is very similar. Thus, data for all weekdays is used here for fitting the splines.

5 Model performance

In order to assess the effect of including occupancy, headway and speed as exogenous regressors on the accuracy of the forecasts provided by the LMDM, various models were compared for several separate subsets of sites in the Manchester network. In particular, forecast models were run for:

- all root nodes;
- four separate bivariate time series formed by the four root nodes together with one of their children;
- four separate trivariate time series formed by the four root nodes together with one of their children and one grandchild.

The reason for this approach was to evaluate the inclusion of predictor variables at a root node on the flow forecasts of its descendants in the DAG.

In the absence of expert information, historical data from July and August 2010 were used to elicit priors. The priors used were comparable across models so that, for example, the spline parameters $\beta_{t1}, \dots, \beta_{tM}$ representing the daily cycle for a series $Y_t(i)$, used the same priors for all models for that series, and so on. These historical data were also used to estimate the basis functions for all splines used in the models. The observation variance $V_t(i)$ was modelled for each $Y_t(i)$ using (4), with, for each model, $\phi_t(i)$ being estimated as usual using the discounting variance learning techniques. For each series, the parameter α was the same for all models and was calculated using the prior data. Once again, all discount factors for all models and series were set to be 0.99. On-line one-step ahead forecasts were then obtained for Wednesday flows from September to October 2010.

5.1 Root nodes

For each of the root nodes, five (univariate) DLMS were considered:

- Model D (daily cycle model) only uses the daily cycle patterns to forecast flows at time t , modelled via splines as described in Section 3;

TABLE 2 ABOUT HERE

- Model O is Model D with the addition of the single predictor variable occupancy at time $t - 1$, modelled via splines as described in Section 4;
- Model S is Model D with the addition of the single predictor variable speed at time $t - 1$, modelled via splines as described in Section 4;
- Model H is Model D with the addition of the single predictor variable headway at time $t - 1$, modelled via splines as described in Section 4;
- Model F (full model) uses cubic splines to model the daily cycle patterns and also uses cubic splines for occupancy, headway and speed measurements at time $t - 1$ to forecast flows as described in Section 4.

Table 2 gives the LPL for each of these models for all the root nodes. All the models with the daily cycle pattern and one single predictor variable (Models O, S and H) provide better forecasts than Model D, with Model H being the best one for almost all sites. When comparing these models with Model F, Models H and O provide slightly better forecasts for site 9206B and Model H also shows a marginal improvement over Model F for 6013B, whereas Model F is the best among all models for sites 9188A and 1431A. A model using Model D with the inverse of headway was also considered (since this variable can be viewed as the inverse of flow and that is also suggested by the scatterplots in Figure 3), but gave worse performance compared to model H.

Although Model F does not necessarily gives the best forecasts for all sites, as mentioned in Section 4.1, from a traffic modelling perspective it is sensible to retain all the variables in the model.

5.2 Children and grandchildren of the root nodes

In order to assess the effects of including predictor variables for root nodes and children, forecasts were obtained using LMDMs for the same four (separate) bivariate series that were considered in Table 1. For each bivariate series, three LMDMs were considered:

- Model D/D uses Model D for both root node and child;

TABLE 3 ABOUT HERE

- Model F/D uses Model F for root node and Model D for child;
- Model F/F uses Model F for both root node and child.

To also evaluate the effect of considering parent flows when forecasting flows of children, independent DLMS using all predictor variables (for both parent and child) were also fitted for each of the bivariate series. The LPLs for all of these models are shown in Table 3.

From Table 3 it is clear that Model F/F is the best model among all possible alternatives for each bivariate series. What’s more, Model F/F provides better forecasts than independent DLMS using all predictor variables for each of the bivariate series. Thus, the inclusion of parent information in addition to the predictor variables when forecasting a child, is better than simply including the predictor variables.

Notice also that Model F/D provides better forecasts when compared to Model D/D for all bivariate series in Table 3. Thus, using the predictor variables in the LMDM seems to improve not only the forecasts at the same site that occupancy, headway and speed were measured, but also affects the quality of the forecasts of its descendants in the DAG.

Similar conclusions can be made when looking at trivariate time series forecasts based on results from Table 4, which shows LPLs for LMDMs for series formed by root nodes together with one of their children and one of their associated grandchildren. In this case, model F/D/D, for example, means an LMDM for a trivariate time series using Model F for root node and Model D (with parents as regressors) for its child and grandchild.

TABLE 4 ABOUT HERE

As another illustration of model improvement when considering occupancy, headway and speed for flow forecasting, Figure 4 shows the observed flows on a specific day for site 9200B, together with forecast means and one-step ahead forecast limits (forecast mean $\pm 2 \times$ forecast standard deviation). The forecasts were calculated considering LMDMs D/D and F/F for the bivariate time series $(Y_t(9206B), Y_t(9200B))$. The F/F model has narrower forecast limits than the D/D model for the whole day, which is an indication that the inclusion of the predictor variables in the model decreases the uncertainty about flows when compared to an LMDM modelling the daily cycle alone. Notice also that the F/F model captures

the deviations from the usual flow patterns that occur during the periods 07:30-08:30 and 15:00-17:00, providing much more accurate forecasts than the D/D model. These periods correspond to peak times in the network, times when in fact flow forecasting models are most useful.

In Figure 4, most observations lie within their respective forecast limits. This should happen for approximately only 95% of observations in a well-calibrated model. Over the whole forecast period, both daily cycle (D) and full (F) models are well-calibrated for the root nodes with roughly 95% of observations lying within the forecast limits for each series. When forecasting child variables as well, however, Model D/D overestimates the forecast uncertainty with roughly 99% to 100% of observations falling within the forecast limits for each series, while this time model F/F is well-calibrated with a coverage of roughly 95%. A similar behaviour was observed for models D/D/D and F/F/F when including grandchild variables. This suggests that, for child and grandchild variables, there are factors affecting the flow variation that are captured by the inclusion of extra variables as predictors in the model.

FIGURE 4 ABOUT HERE

6 Final remarks

The methodology proposed in this paper tackles both the problem of using extra traffic variables for enhancing flow forecasts, whilst also accommodating, and taking advantage of, the multivariate nature of the problem to provide real-time multivariate flow forecasts. Neither of these issues are often considered in traffic modelling.

The performance of all models presented here was based on past traffic data. However, when using the LMDM in an on-line environment in practice, on-line model monitoring would be crucial in order to monitor how well the model is performing over time, as well as to identify when model intervention is required (the technique of intervention allows information regarding a change in the time series to be fed in the model to maintain forecast performance — see Queen and Albers, 2009). Given that the LMDM is a set of (conditional) DLMS, it should be relatively straightforward to adapt established monitoring and intervention techniques for DLMS (as described in West and Harrison, 1997) into the LMDM context.

References

- Abdulhai, B., Porwal, H. and Recker, W. (1999). Short-term Freeway Traffic Flow Prediction Using Genetically-optimized Time-delay-based Neural Networks. *In: Proceedings of the 78th Annual Meeting of the Transportation Research Board*. National Academies Press, Washington, DC.
- Ahmed, M. S. and Cook, A. R. (1979). Analysis of freeway traffic time-series data by using Box-Jenkins techniques, *Transportation Research Record*, **773**, 47-49.
- Anacleto, O., Queen, C.M. and Albers, C.J. (2013). Multivariate forecasting of road traffic flows in the presence of heteroscedasticity and measurement errors. *Applied Statistics*, **62**, Part 2.
- Ashton, W.D. (1966). *Theory of Road Traffic Flow*. Methuen's Monographs on Applied Probability and Statistics. John Wiley, London.
- Chandra, S.R. and Al-Deek, H. (2009). Predictions of Freeway Traffic Speeds and Volumes Using Vector Autoregressive Models *Journal of Intelligent Transportation Systems*, **13**, 53-72.
- Clark, S. (2003). Traffic prediction using multivariate non-parametric regression. *Journal of Transportation Engineering*, **129(2)**, 161-168.
- Gilmore, J.F., and Abe, N. (1995). Neural network models for traffic control and congestion prediction. *Journal of Intelligent Transportation Systems*, **3**, 231-252.
- Greenshields, B.D (1935). A study of traffic capacity. *Highway Research Board Proceedings*, **14**, 448-474.
- Harrell, F.E. (2001). *Regression modelling strategies with applications to linear models, logistic regression and survival analysis*. Springer-Verlag, New York.
- Hastie, T., Tibshirani, R., and Friedman, J. (2001). *The Elements of Statistical Learning*. Springer-Verlag, New York.
- Innamaa, S. (2000). Short-term prediction of traffic situation using MLP-neural networks, *in: Proceedings of the 7th World Congress on Intelligent Transportation Systems*, Turin, Italy.
- Kamarianakis, Y., and Prastacos, P. (2005). Space-time Modeling of Traffic Flow. *Computers & Geosciences*, **31**, 119-133.
- Levin, M. and Tsao, Y.D. (1980). On forecasting freeway occupancies and volumes. *Transportation Research Record*, **773**, 47-49.
- Li, B. (2009). A Non-Gaussian Kalman Filter With Application to the Estimation of Vehicular Speed. *Technometrics*, **51**, 162-172.
- Petris, G., Petrone, S. and Campagnoli, P. (2009). *Dynamic Linear Models With R*. Springer, New York.

- Prado, R., and West, M. (2010). *Time Series: modelling, Computation and Inference*. Chapman & Hall, New York.
- Queen, C.M. and Smith, J.Q. (1993). Multiregression dynamic models. *Journal of the Royal Statistical Society, B*, **55**(4), 849-870.
- Queen, C.M., Wright, B.J. and Albers, C.J. (2007). Eliciting a Directed Acyclic Graph for a Multivariate Time Series of Vehicle Counts in a Traffic Network. *Australian and New Zealand Journal of Statistics*, **49**(3) , 221-239.
- Queen, C.M., Wright, B.J. and Albers, C.J. (2008). Forecast covariances in the linear multiregression dynamic model. *Journal of Forecasting*, **27**, 175-191.
- Queen, C.M. and Albers, C.J. (2009). Intervention and Causality: Forecasting Traffic Flows Using a Dynamic Bayesian Network. *Journal of the American Statistical Association*, **104**, 669-681.
- Stathopoulos, A. and Karlaftis, G.M. (2003). A multivariate state space approach for urban traffic flow modelling and prediction. *Transportation Research Part C*, **11** (2), 121-135.
- Sun, S. L., Zhang, C. S., and Yu, G. Q. (2006). A Bayesian Network Approach to Traffic Flows Forecasting. *IEEE Transactions on Intelligent Transportation Systems.*, **7**, 124-132.
- Tebaldi, C., West, M. and Karr, A.K. (2002). Statistical analyses of freeway traffic flows. *Journal of Forecasting*, **21**, 39-68.
- Vlahogianni, E. I., Golias, J. C. and Karlaftis, M. G. (2004). Short-term traffic forecasting: Overview of objectives and methods. *Transport Reviews*, **24**(5), 533-557.
- West, M. and Harrison, P.J. (1997). *Bayesian Forecasting and Dynamic Models* (2nd edition) Springer-Verlag, New York.
- Whittaker, J., Garside, S. and Lindveld, K. (1997). Tracking and predicting a network traffic process. *International Journal of Forecasting*, **13**, 51-61.

Table 1: LPLs for LMDMs with different seasonal representations.

Bivariate series	LMDM		
	seasonal factors	static splines	dynamic splines
$Y_t(9206B), Y_t(9200B)$	-8,794	-8,857	-8,570
$Y_t(6013B), Y_t(6007L)$	-8,159	-8,157	-7,886
$Y_t(9188A), Y_t(9193J)$	-8,581	-8,647	-8,336
$Y_t(1431A), Y_t(1437A)$	-9,056	-8,839	-8,597

Table 2: LPLs for various models for all root nodes of the Manchester network.

Model	Root node			
	$Y_t(9206B)$	$Y_t(6013B)$	$Y_t(9188A)$	$Y_t(1431A)$
Daily cycle model (D)	-8,259	-7,182	-8,362	-8,128
O	-8,077	-7,138	-8,068	-7,913
S	-8,162	-7,165	-8,141	-7,966
H	-8,075	-7,127	-8,025	-7,931
Full model (F)	-8,084	-7,128	-8,003	-7,887

Table 3: LPLs for different LMDMs for bivariate time series from the Manchester network.

Bivariate series	LMDM			Independent DLMS, each using all predictor variables
	D/D	F/D	F/F	
$Y_t(9206B), Y_t(9200B)$	-15,156	-15,064	-14,986	-15,467
$Y_t(6013B), Y_t(6007L)$	-13,620	-13,559	-13,520	-13,852
$Y_t(9188A), Y_t(9193J)$	-14,591	-14,219	-14,208	-14,517
$Y_t(1431A), Y_t(1437A)$	-15,163	-14,862	-14,817	-15,402

Table 4: LPLs for different LMDMs for trivariate time series from the Manchester network

Trivariate series	LMDM			Independent DLMS, each using all predictor variables
	D/D/D	F/D/D	F/F/F	
$Y_t(9206B), Y_t(9200B), Y_t(9189B)$	-21,935	-21,811	-21,741	-22,740
$Y_t(6013B), Y_t(6007L), Y_t(6004L)$	-19,033	-18,972	-18,923	-19,566
$Y_t(9188A), Y_t(9193J), Y_t(1436M)$	-20,207	-19,791	-19,764	-20,598
$Y_t(1431A), Y_t(1437A), Y_t(1441A)$	-21,879	-21,509	-21,426	-22,418

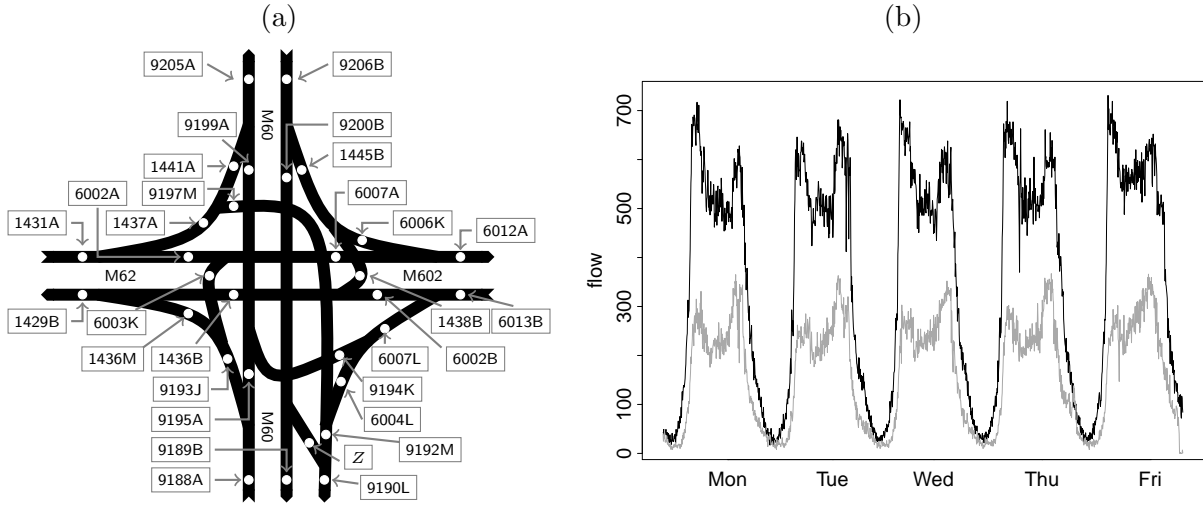


Figure 1: (a) Schematic diagram of the Manchester network. (b) 5-minute flows for site 9206B (black line) and 1437A (grey line) for 4–8 October 2010.

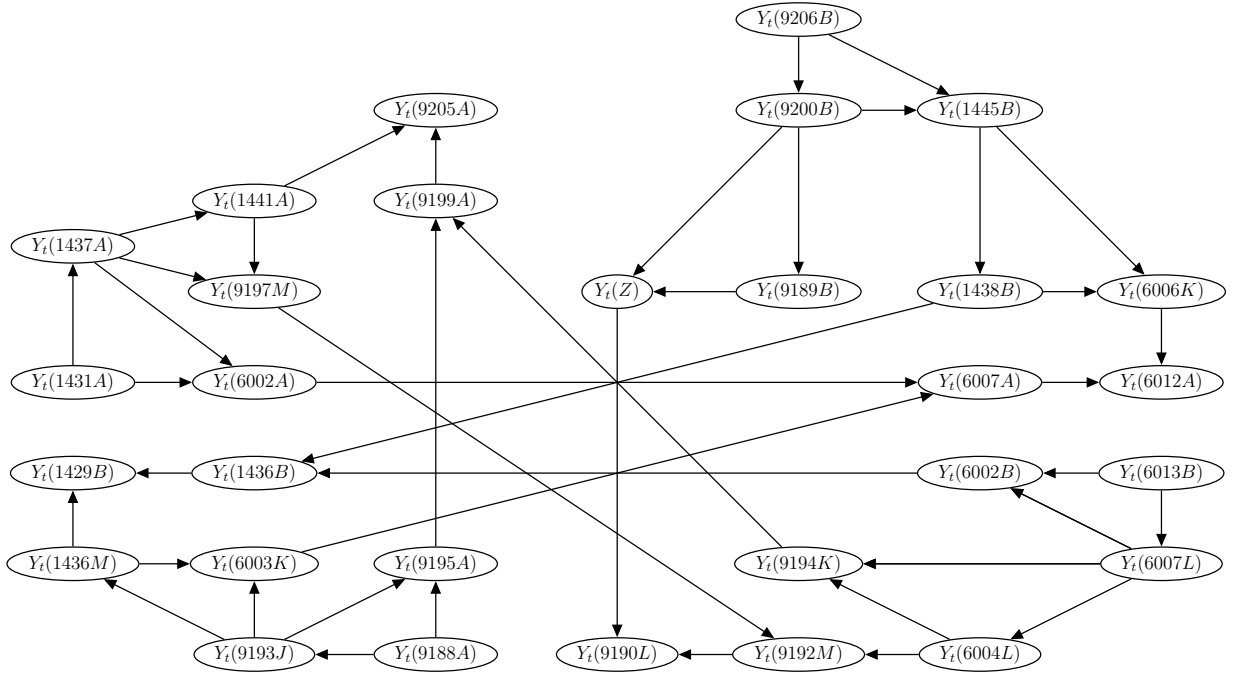


Figure 2: Elicited DAG for the Manchester network used in Anacleto *et al.* (2013).

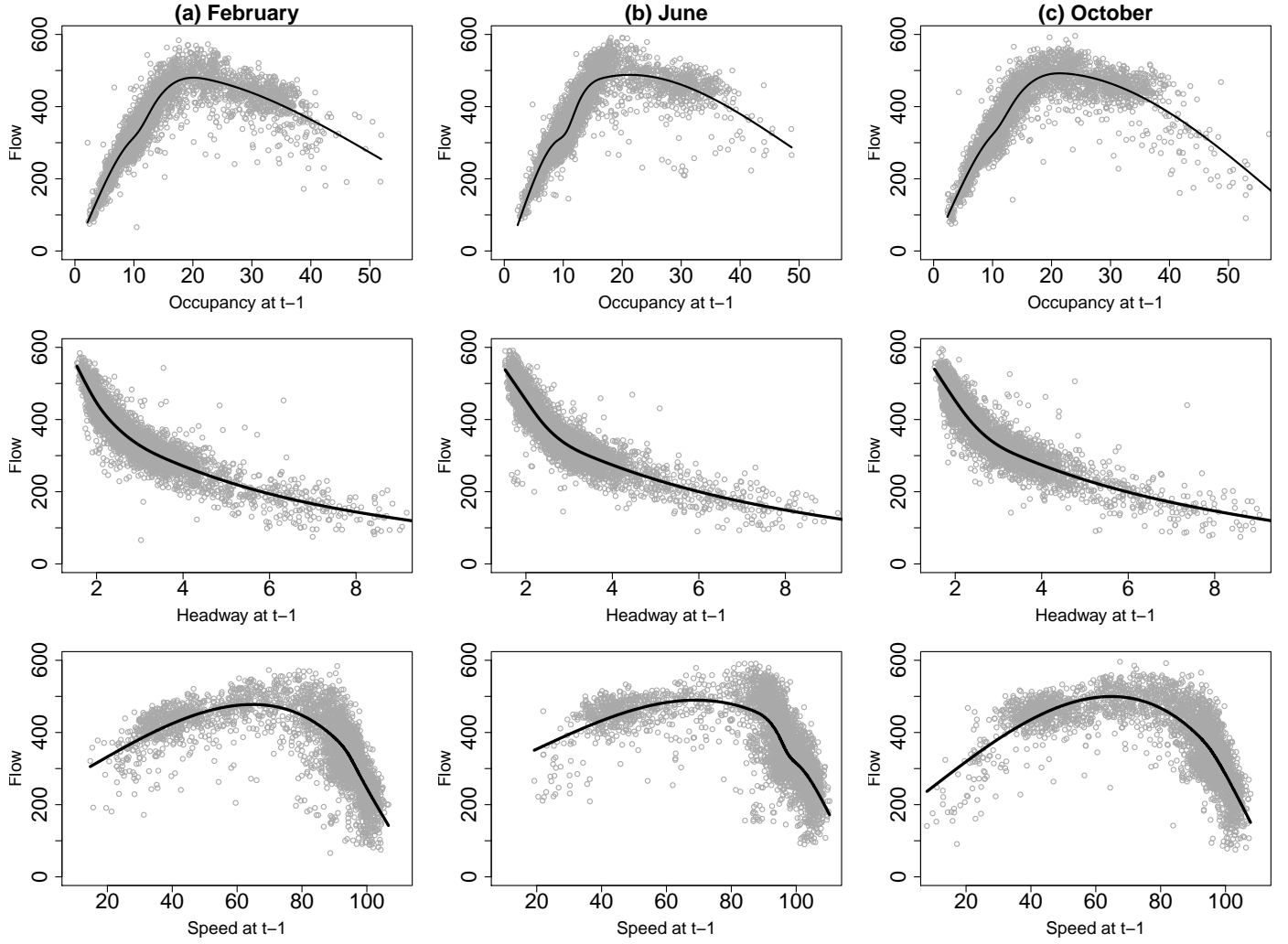


Figure 3: Scatterplots of flows at site 9188A at time t versus occupancy, headway and speed at $t - 1$, in (a) February, (b) June and (c) October 2010.

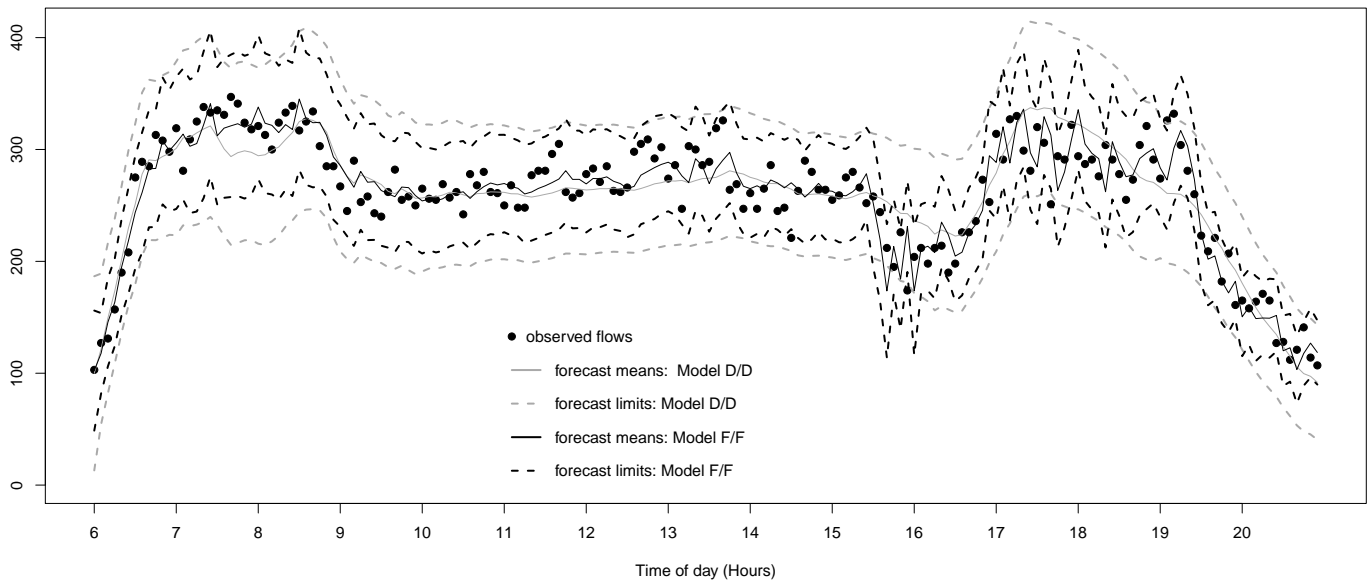


Figure 4: Observed flows at site 9200B on 27 October 2010, along with forecast means and forecast limits based on LMDMs D/D and F/F for bivariate series $(Y_t(9206B), Y_t(9200B))$.